Validation of a method to differentiate arterial and venous vessels in CT perfusion data using linear combinations of quantitative time-density curve characteristics

Lukas Havla[1], Moritz Schneider[1], Kolja M. Thierfelder[2], Sebastian E. Beyer[2], Birgit Ertl-Wagner[2], Wieland H. Sommer[2], Olaf Dietrich[1]

[1] Josef Lissner Laboratory for Biomedical Imaging, Institute for Clinical Radiology, Ludwig-Maximilians-University Hospital Munich, Germany

[2] Institute for Clinical Radiology, Ludwig-Maximilians-University Hospital Munich, Germany

ELECTRONIC PREPRINT VERSION:
Not for commercial sale or for any systematic external distribution by a third party

Final version: *Eur Radiol.* 2015; **25**(10): 2937–2944. <URL:http://dx.doi.org/10.1007/s00330-015-3709-0>

Abstract

Objectives: To develop and evaluate a new method that reliably differentiates between cerebral arteries and veins using voxel-wise CT-perfusion-derived parameters.

Materials and Methods: Fourteen consecutive patients with suspected stroke but without pathological findings were examined at a multi-detector CT system: 32 dynamic phases (Δt = 1.5 s) during application of 35 mL iomeprol-350 were acquired at 80kV/200mAs. Three hemodynamic parameters were calculated for 18 arterial and venous vessel segments: *A* (maximum of the time-density-curve), *T* (time-to-peak), and *W* (full-width-at-half-maximum). Using receiver-operator-characteristic (ROC) curve analysis and Fisher's linear discriminant analysis (FLDA), the performance of every classifier (*A, T, W*) and of all linear combinations for the differentiation of arterial and venous vessels was determined.

Results: A maximum area under the ROC-curve (AUC) of 0.945 (accuracy=86.8 %) was obtained using the FLDA combination of *A&T* or the triplet FLDA of *A&T&W* for the classification of venous and arterial vessels. The best single parameter was *T* with an AUC of 0.871 (accuracy=79.0 %), which performed significantly worse than the combination *A&T* (*P*<0.001).

Conclusions: Arteries and veins can be accurately differentiated based on dynamic CT perfusion data using the maximum of the time-density curve, its time-to-peak, its width and, in particular, FLDA combinations of these parameters, which yield accuracies up to 87 %.

Key points

1) For classification of cerebral vasculature, time-to-peak has the best single-parameter accuracy.
2) Fisher's linear discriminant analysis improves the performance of the individual classifiers.
3) Combining signal maximum and time-to-peak parameters significantly increased the classifying potential.
4) Pre-processing of time-density-curves by Gaussian filtering or fitting can improve diagnostic accuracy.

Keywords

X-ray computed tomography, Diagnostic imaging, Angiography, Discriminant analysis, Brain, CT perfusion, Ischemic stroke

Corresponding author:

Lukas Havla
Josef Lissner Laboratory for Biomedical Imaging
Institute for Clinical Radiology
Ludwig-Maximilians-University Hospital Munich
Marchioninistr. 15, 81377 Munich, Germany
E-mail: lukas.havla@med.uni-muenchen.de

Introduction

In computed tomography angiography (CTA) of intracranial vessels, a concomitant enhancement of both arteries and veins is often seen at the time point of acquisition. In conventional single-phase CTA, the predominant visualization of the arterial [1], arteriovenous [2], and venous [3] cerebral vasculature depends on the time delay after injection of a contrast-agent bolus. A previously described drawback of conventional CTA is its potential failure to capture delayed collateral enhancement [4].

Several studies demonstrated the value of the acquisition and post-processing of multiple time frames and, in particular, of CT perfusion datasets, to assess the maximal extent of collateralization [5–7] or to define the infarct and penumbra [8, 9]. However, the differentiation between arteries and veins, and especially the venous superimposition when assessing the arterial vasculature, remain a major problem in delay-insensitive CTA approaches [10].

A commonly used marker to differentiate between arterial and venous vessels is the time-to-peak (TTP) parameter [11, 12], which measures the duration until the time-density curve peaks. In general, TTP is longer for venous vessels than for arteries in an organ. This parameter, however, does not differentiate between rapid bolus dilation in the capillaries and continuing intra-vascular bolus propagation.

Other semi-quantitative characteristics, which can be derived from CT perfusion data, such as the maximum or the slope of the time-density curve, the area under the curve (AUC), or recently [13] the full-width-at-half-maximum (FWHM) of the time-density curve may be expected to help differentiate arterial and venous vessels.

The purpose of the present study was to develop and evaluate a new method for the improved differentiation of cerebral arteries and veins using the attenuation maximum, TTP, and FWHM derived voxel-wise from CT perfusion datasets.

Material and Methods

Patient population

This study was approved by the institutional review board and informed consent was waived. Fifteen consecutive patients with CT examinations between December 22, 2012 and February 1, 2013 were selected for this retrospective study. Inclusion criteria were suspected acute stroke and the availability of whole-brain CT perfusion data. We specifically excluded patients with any pathological finding on non-enhanced CT, CTA, CTP or follow-up MRI. One patient had to be excluded due to non-standard bolus injection. The final cohort of 14 patients (mean 73 years, range 17-97) comprised six females.

Data acquisition

Examinations were performed with a dual-source CT system (SOMATOM Definition Flash, Siemens Healthcare, Forchheim, Germany) in single-source mode. 99 slices (total slab thickness 99 mm, slice thickness = 1.5 mm, slice increment = 1.0 mm) were continuously acquired over 48 seconds in table shuttle mode within 32 sweeps. The resulting mean time interval between consecutive slab acquisitions is 1.5 s. Tube voltage and tube current were set to 80 kV and 200 mAs, respectively, yielding dose exposure of $CTDIvol_{16cm} = 276.21$ mGy. The total amount of iomeprol-350 (Imeron 350, Bracco Imaging, Konstanz, Germany) was 35 mL injected at a flow rate of 4.5 mL/s prior to a saline flush of 40 mL (at the same rate).

Data processing

For all post-processing tasks, a standard PC equipped with 16 GB RAM and a conventional Intel i5 processor was used. Initial rigid-body motion correction of the CT perfusion datasets was performed with the open source elastix toolbox [14] using a binary mask containing all pixels with density > 0 HU at $T = 0$. Subsequently, all 32×99 (phases × slices) CT DICOM images were imported into an in-house developed software (PMI, Platform for Medical Imaging v0.4 [15]).

All statistical calculations were performed using R (v3.1.0; R Foundation for Statistical Computing, Vienna, Austria [16]). Receiver Operating Characteristic (ROC) curve analysis was performed with the open-source R package *pROC* [17].

Study design and statistical evaluation

The study was performed in two steps separating (1) the voxel-wise calculation of three hemodynamically characteristic parameters derived from the acquired time-density curves, and (2) the statistical combination and evaluation of these parameters. Both steps are based on the parameter evaluation in a set of either arterial or venous regions of interest (ROIs); the classification performance was always assessed using ROC curve analyses.

Vascular regions of interest

A total of 18 regions of interest (ROIs) with varying size (29.9±30.0 voxels) were defined in each subject adapted to the individual cerebral vessel anatomy in 11 arteries (2× internal carotid / 1× basilar / 2× M1 middle cerebral / 2× P1 posterior cerebral / 2× M2 middle cerebral / 2× leptomeningeal collaterals) and 7 venous vessels (1× sagittal sinus / 2× transverse sinus / 2× sigmoid sinus / 2× bridging veins to the sagittal sinus).

Hemodynamic parameters

Three hemodynamically characteristic parameters were calculated voxel-by-voxel (i. e., as 3D parameter maps) from the acquired time-density curves as visualized in Figure 1:

1) the maximum of the time-density curve (also used as angiographic image intensity)
2) the TTP defined as the position of the time-density curve maximum
3) the FWHM describing the bolus width (determined after linear curve interpolation).

For statistical analysis, the parameter mean values in each vessel-segment ROI were calculated for all three parameter maps (maximum, TTP, FWHM). Patient-individual normalization was then performed: every parameter was divided by the mean value in the two carotid arteries of each patient; the resulting normalized parameters were called: *A* (normalized maximum), *T* (normalized TTP), and *W* (normalized FWHM).

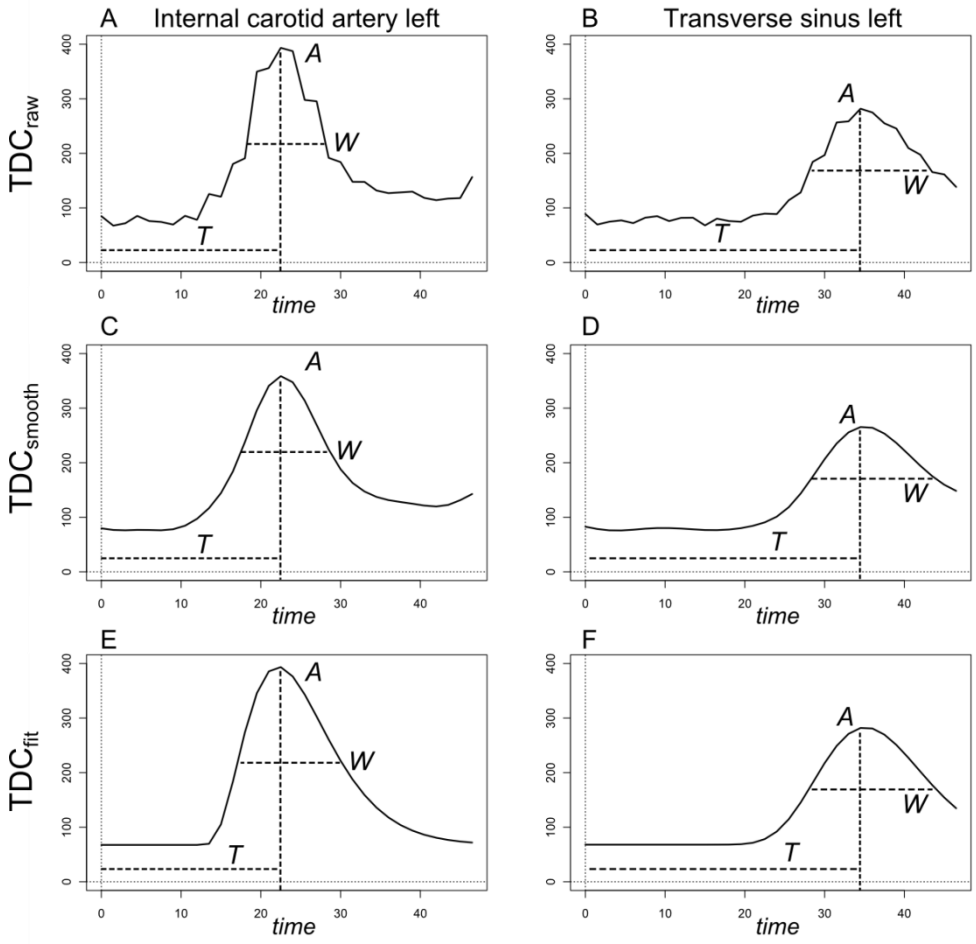

Figure 1. Time-density curve pre-processing and evaluated parameters. Left column shows data of an arterial and right column of a venous vessel. In the top row (A and B), the different hemodynamic parameters (*A, T, W*) are illustrated in unprocessed raw time-density curves. The middle and bottom row (C, D and E, F) display the parameters of the pre-processed signal courses TDC_{smooth} and TDC_{fit}. Exemplary data is taken from a 76 y/o male patient.

Part 1 – Time-density curve pre-processing and parameter calculation

Several strategies exist to derive the three parameters *A, T,* and *W* from the acquired time-density curves (TDCs). In this study, we compared three methods (illustrated in Figure 1) for the calculation of these parameters based on:

1) unprocessed ("raw") time-density curves referred to as TDC_{raw}
2) low-pass filtered time-density curves using temporal Gaussian smoothing with a filter width (standard deviation) of 1.5 s (previously demonstrated to optimize vascular contrast [10]) referred to as TDC_{smooth}
3) gamma-variate fits *f(t)* to each voxel curve a with four free parameters (width ϑ, shape parameter *k*, amplitude *a*, *offset* t_0):

$$f(t) = \frac{\alpha}{\vartheta^k} \cdot \frac{1}{\Gamma(k)} \cdot (t - t_0)^{k-1} \cdot \exp\left(\frac{-(t - t_0)}{\vartheta}\right)$$

$$\Gamma(k+1) = k!$$

TDC_{fit} was then calculated based on this fit function with a temporal resolution of $\Delta t = 0.1$ s; this method is referred to as TDC_{fit}.

TDC_{raw} and TDC_{smooth} were computed voxel-by-voxel for the entire image volume whereas Gamma-variate fits (TDC_{fit}) were only calculated for the vascular regions of interest due to the computational load.

The vascular classification potential of each parameter (*A, T,* and *W*) calculated by these three approaches was then compared based on the area under the ROC curve (AUC). DeLong's test [17, 18] was used to assess the differences between the AUC values of the differently pre-processed time-density curves. The significance level was set to $P = 0.05$. Since more than one statistical test ($m > 1$) was conducted within the same data frame, the Bonferroni correction [19] was applied by setting $P_{corr} = P / m$ (m: number of statistical tests).

Part 2 – Differentiation of arterial and venous vessels

Parameter values (*A, T,* and *W*) from the best pre-processing approach established by comparing TDC_{raw}, TDC_{smooth}, and TDC_{fit} were then used to further optimize the differentiation of arterial and venous cerebral vessels by comparing their individual performance and, in particular, the performance of linear parameter combinations.

The linear combination of two or three parameters was performed with Fisher's linear discriminant analysis (FLDA). FLDA is a statistical method to reduce the dimensionality of data; by finding an optimal linear combination of a given feature set, the differentiation between two (or more) classes can be improved [20–22]. FLDA was applied using either two out of three alternately combined parameters or using all three parameters as input. FLDA is implemented and made available as open-source software in R packages (*Bioconductor* [23] and *CMA* [24]).

Consequently, seven ROC curve analyses were performed: three for every individual parameter, three for the linear combinations of two parameters, and one for the linear combination of all three parameters. Four statistical measures were determined from the ROC curves: 1) AUC 2) accuracy, 3) sensitivity, and 4) specificity based on a threshold minimizing the distance between the ROC curve and the top-left ROC coordinate corner. DeLong's test [17, 18] was used to assess the differences between the ROC curves of the best single and FLDA-combined parameters. The significance level was set to $P = 0.05$.

The pairwise correlation between the three parameters *A*, *T*, and *W* was assessed by calculating linear Pearson correlation coefficients.

Results

Nine of 252 (18 vessel segments × 14 included patients) ROIs were excluded as they were not in the field of view ($N = 3$) or suffered from image registration artifacts in distal slices ($N = 6$). The results were based on 243 individual ROIs, each of which yielded nine (*A, T, W*) parameter mean values.

Part 1 – Time-density curve pre-processing

In Table 1, the AUC values from all ROC curves are listed. For *A* and *T*, the gamma-variate fitted AUC values outperformed those calculated from TDC_{raw} or TDC_{smooth}; for *W*, the AUC of TDC_{smooth} (0.796) was slightly higher than of TDC_{fit} (0.789). The maximum AUC of 0.871 was obtained using *T* and TDC_{fit}.

DeLong's test (with Bonferroni correction for $m = 9$ comparisons) showed 3 significantly differing ROC curves: for the single parameter *A*, TDC_{smooth} resulted in a significantly lower AUC than both other pre-processing strategies ($P < 0.00001$); for the parameter *T*, TDC_{fit} yielded a significantly better AUC than TDC_{smooth} ($P \leq 0.005$).

Overall, the best results were obtained with TDC_{fit}, which was subsequently used for further evaluation.

Part 2 – Differentiation of arterial and venous vessels

AUC as well as accuracy, sensitivity, and specificity at an optimal threshold were calculated for seven ROC curves and the resulting values are summarized in Table 2.

One-parameter ROC curves

The best standalone classifier was *T* with an accuracy of 79.0 % followed by *W* (70.8 %) with respect to the optimal threshold from the ROC curve.

Table 1. Comparison of AUCs of different time-density curve pre-processing approaches.

	AUC (95% confidence interval)		
	TDC_{raw}	**TDC_{smooth}**	**TDC_{fit}**
A	0.666 (0.598 - 0.734)	0.641 (0.572 - 0.710)	**0.669** (0.601 - 0.737)
T	0.823 (0.772 - 0.875)	0.823 (0.773 - 0.873)	**0.871** (0.828 - 0.914)
W	0.748 (0.686 - 0.809)	**0.796** (0.738 - 0.854)	0.789 (0.731 - 0.847)

Bold numbers indicate highest AUC values.
A (normalized maximum), *T* (normalized time-to-peak), *W* (normalized full-width-at-half-maximum), TDC (time density curve), AUC (area-under-the-curve)

Table 2 Results from statistical analysis of TDC_{fit} classifiers.

	AUC (95% conf. int.)	accuracy [%]	sensitivity [%]	specificity [%]	Threshold for venous vessels
A	0.669 (0.601 - 0.737)	60.1	39.9	91.6	$A < 0.664$
T	0.871 (0.828 - 0.914)	79.0	66.9	97.9	$T > 1.087$
W	0.789 (0.731 - 0.847)	70.8	59.5	88.4	$W > 1.108$
A & T	**0.945** (0.921 - 0.970)	**86.8**	86.5	87.4	$-0.183 \times A + 0.229 \times T > 0.109$
A & W	0.809 (0.754 - 0.865)	73.3	62.8	89.5	$-0.169 \times A + 0.167 \times W > 0.060$
T& W	0.896 (0.858 -0.934)	81.1	70.9	96.8	$0.217 \times T + 0.043 \times W > 0.279$
A & T& W	**0.945** (0.920 - 0.970)	**86.8**	86.5	87.4	$-0.184 \times A + 0.232 \times T - 0.005 \times W > 0.107$

Bold numbers indicate highest statistical measures.
A (normalized maximum), *T* (normalized time-to-peak), *W* (normalized full-width-at-half-maximum), TDC (time density curve), AUC (area-under-the-curve)

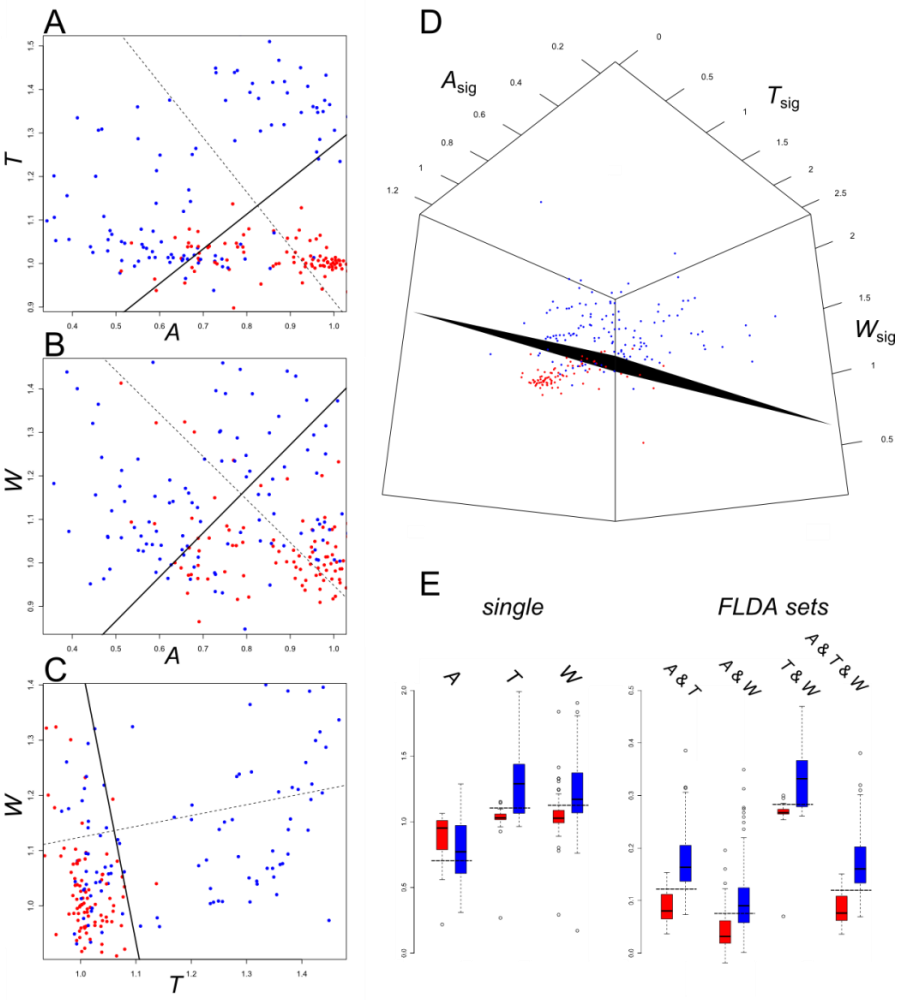

Figure 2. Classification plots using TDC_{fit} data. Arterial data are shown in red, venous in blue. The two-parameter Fisher's Linear Discriminant Analysis (FLDA) plots are shown in A-C (for purpose of better visualization only the 5th to the 95th percentile of the data is plotted). The dashed line constitutes the normal to the respective discriminant hyperplane whereas the solid line represents the optimal threshold as determined by the subsequent ROC curve analysis. D contains the 3D plot of the triplet FLDA (in black the hyperplane). E shows boxplots of all three single parameters and seven parameter combinations (optimal thresholds as dashed line). The boxplot of the three-parameter FLDA combination and *A* & *T* visualize very good discrimination between arterial and venous vessels.

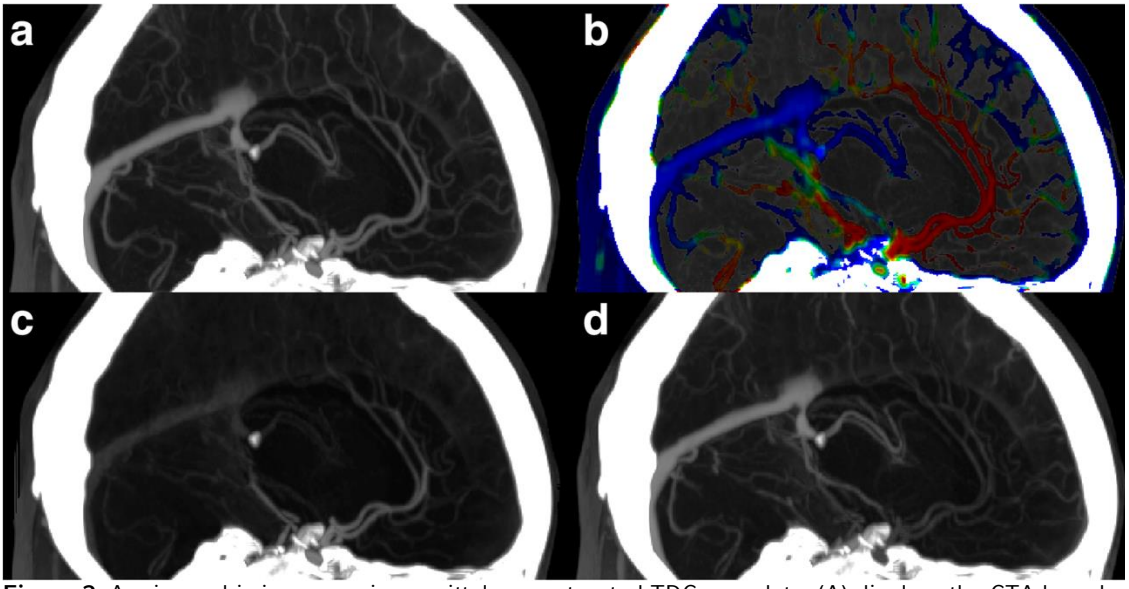

Figure 3. Angiographic images using sagittal reconstructed TDC_{smooth} data. (A) displays the CTA based on the parameter *A*. (B) shows the CTA superimposed with the FLDA parameter combination of *A* & *T* color-coded from red to blue. Arteries are coded to be red, veins blue, and vessels with intermediate classifier are shown in green. At the bottom, one predominantly arterial (C) and one predominantly venous (D) image is shown. The differentiation is based on the FLDA parameter combination of *A* & *T*. Patient data is taken from a 17 y/o male.

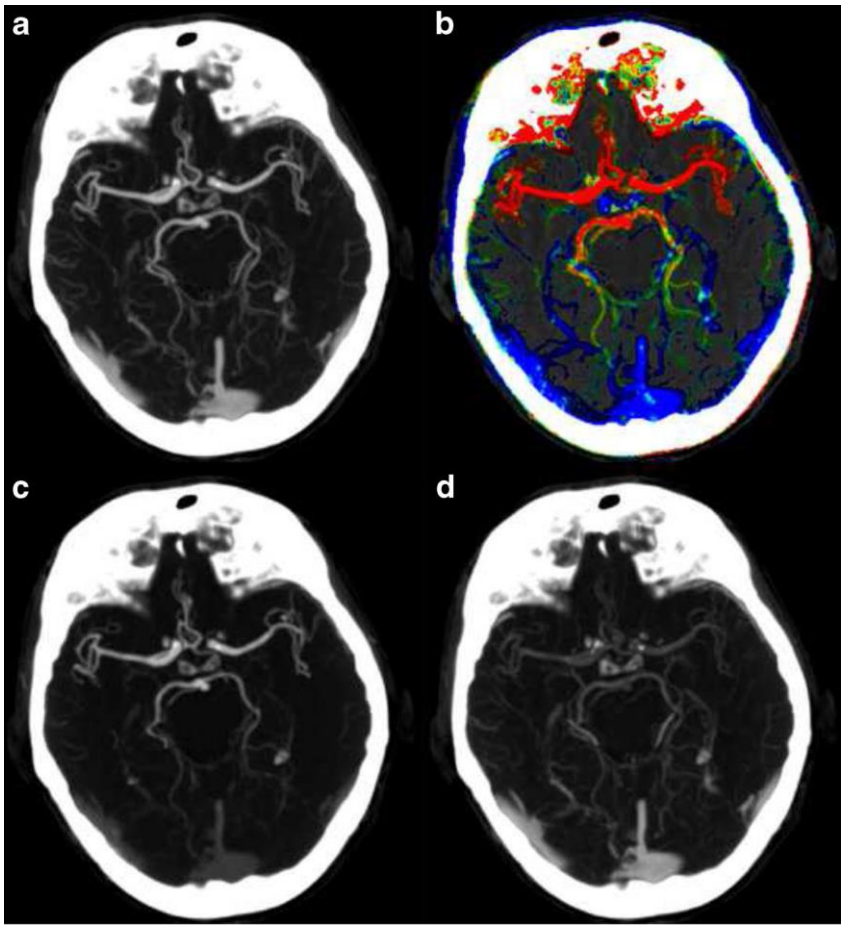

Figure 4. Angiographic images using transversal TDC_{smooth} data. (A) displays the CTA of the parameter *A*. (B) shows the CTA superimposed with the FLDA parameter combination of *A* & *T* color-coded from red to blue.. Arteries are coded to be red, veins blue, and vessels with intermediate classifier are shown in green. At the bottom, one predominantly arterial (C) and one predominantly venous (D) image is shown. The differentiation is based on the FLDA parameter combination of *A* & *T*. Patient data is taken from a 87 y/o male.

FLDA results

Three linear FLDA combinations of two parameters were tested as classifiers for arterial vs. venous vessels using ROC curves. The highest accuracy of 86.8 % (AUC of 0.945) was obtained with the pair *A* & *T*. The combination of *T* & *W* (accuracy: 81.1 %, AUC: 0.896) was ranked second. The linear FLDA combination of all three parameters yielded the same maximal accuracy (86.8 %) and AUC (0.945) as the combination *A* & *T*. Thus, *A* & *T* and *A* & *T* & *W* outperformed all other test classifiers; the obtained sensitivity was 86.5 % at a specificity of 87.4 %.

Comparing the ROC curves of the best single parameter *T* (AUC = 0.871) and the best linear combination *A* & *T* (AUC = 0.945) revealed a highly significant difference (p = 0.0002).

Threshold values which optimally separate arterial and venous vessels are graphically illustrated in Figure 2 and are also provided in Table 2.

Pairwise Pearson's linear correlation coefficients between the evaluated parameters were low for all combinations. Whereas correlation was found to be *poor* for *A* vs. *T* ($r = 0.22$) and *moderate* for *T* vs. *W* ($r = 0.52$), Pearson's r was negative for *A* vs. *W* ($r = -0.09$) and indicated no correlation.

In Figure 3 and 4, angiographic images are shown. *A* was interpreted as angiographic intensity information. All images were color-coded from red (arterial) to blue (venous) using the (optimal) 2-parameter FLDA classifier.

Discussion

The purpose of the present study was to develop and evaluate a new method to reliably differentiate

between cerebral arteries and veins using three normalized CT perfusion derived parameters: attenuation maximum (*A*), TTP (*T*), and FWHM (*W*). Our results show that cerebral arterial and venous vessels can be differentiated with varying accuracy depending on the calculation, selection, and number of parameters. To our knowledge, this is the first study to systematically differentiate arteries and veins using CT perfusion data characteristics in combination with Fisher's linear discriminant analysis.

For classification of cerebral vasculature, the best result using only a single parameter was achieved by *T*, followed by *W* and by *A* with lowest classification results. Using two parameters, the best results were observed when combining *T* with *A*. The results obtained by this parameter set did not differ from those achieved by a three-parameter FLDA combination. Overall, the application of FLDA always increased the performance of the individual classifiers; the difference between the ROC curves of the best single parameter *T* and the FLDA combination of *A* & *T* was highly significant ($P < 0.001$).

Due to broadening effects, the peak value of the time-density curve decreases noticeably in venous vessels (cf. boxplot of *A* in Figure 2); however, the signal intensities alone are not very specific or sensitive as classifiers because there is a natural variation of the contrast-enhancing tracer amount between narrow and wide vessels. The FLDA combination of *A* with *T* results in a substantially higher AUC value (0.945) in contrast to joining *T* and *W* without *A* (0.896). Apparently, Fisher's linear discrimination analysis exploits the potential of two analytically unrelated parameters. Low Pearson's *r* correlation coefficients between the evaluated parameters agree with the assumption that the parameters can be considered as independent input.

The initial comparison of three pre-processing algorithms demonstrated superiority of the TDC_{fit} parameters: gamma-variate fitting with 4 free parameters improved the AUC values for 2 out of 3 statistical measures. However, the simpler approaches TDC_{raw} and TDC_{smooth} resulted in good AUC values as well; thus, time-density curve preprocessing without the relatively complex fitting algorithm also appears justified.

Beyond vessel classification, the method of combining several signal-course characteristics can potentially improve the suppression of venous superimposition in angiographic data sets. Venous superimposition often complicates the assessment of the arterial vasculature, especially in the setting of acute stroke [10]. Given that CT perfusion is already performed in a patient, the presented approach including color-coded images (c.f. Figure 3 and 4) does not require extra image acquisitions or contrast agent administration.

Intracranial venous thromboses are often diagnosed late due to their unspecific clinical presentation and commonly subtle imaging findings (2). In this context, the presented method could be used to selectively construct venographies and to minimize arterial superposition.

The following limitations of the study need to be taken into account when interpreting the data: 1) The sample size was relatively small. 2) The data was acquired in table shuttle mode, however, our software was not capable to utilize slice-specific acquisition times. Thus, it was assumed that the mean time resolution of 1.5 s is valid independent of the slice *z*-position. 3) The study's design was retrospective. Further prospective studies are necessary to confirm these results. 4) This study did not assess the therapeutic impact of the proposed method. Further research should analyze the utility of this method in the decision of thrombolysis with acute stroke patients. 5) The precise individual axial coverage varied slightly due to technical limitations: therefore predominantly *central* vessels had to be included in our analysis.

In patients with ischemic stroke, collateral blood flow has been determined as a predictor both for final infarct volume [25] and for a favorable clinical outcome [26]. To capture collateral blood flow delayed acquisition is needed; this leads to an impaired differentiation of leptomeningeal collaterals and bridging veins. Future work will need to investigate whether this proposed technique has the potential to influence clinical decision making by quantified differentiation between leptomeningeal collaterals and bridging veins.

In conclusion, our results show that arterial and venous vessels can be accurately differentiated based on dynamic CT perfusion data using the maximum (*A*) of the time-density curve, its time to peak (*T*), its width (*W*) and, in particular, FLDA combinations of these parameters, which yield accuracies up to 87 %. The predominant single characteristic providing the best performance is the normalized time-to-peak parameter (*T*).

References

1. Menon BK, Smith EE, Modi J, et al. (2011) Regional leptomeningeal score on CT angiography predicts clinical and imaging outcomes in patients with acute anterior circulation occlusions. AJNR Am J Neuroradiol 32:1640–5. doi: 10.3174/ajnr.A2564
2. Klingebiel R, Zimmer C, Rogalla P, et al. (2001) Assessment of the arteriovenous cerebrovascular system by multi-slice CT. A single-bolus, monophasic protocol. Acta Radiol 42:560–2.
3. Casey SO, Alberico RA, Patel M, et al. (1996) Cerebral CT venography. Radiology 198:163–70. doi: 10.1148/radiology.198.1.8539371
4. Prokop M (2000) Multislice CT angiography. Eur J Radiol 36:86–96.
5. Calleja AI, Cortijo E, García-Bermejo P, et al. (2013) Collateral circulation on perfusion-computed tomography-source images predicts the response to stroke intravenous thrombolysis. Eur J Neurol 20:795–802. doi: 10.1111/ene.12063
6. Smit EJ, Vonken E, van Seeters T, et al. (2013) Timing-invariant imaging of collateral vessels in acute ischemic stroke. Stroke 44:2194–9. doi: 10.1161/STROKEAHA.111.000675
7. Frölich AMJ, Wolff SL, Psychogios MN, et al. (2014) Time-resolved assessment of collateral flow using 4D CT angiography in large-vessel occlusion stroke. Eur Radiol 24:390–6. doi: 10.1007/s00330-013-3024-6
8. Wintermark M, Flanders AE, Velthuis B, et al. (2006) Perfusion-CT assessment of infarct core and penumbra: Receiver operating characteristic curve analysis in 130 patients suspected of acute hemispheric stroke. Stroke 37:979–985. doi: 10.1161/01.STR.0000209238.61459.39
9. Wintermark M, Sesay M, Barbier E, et al. (2005) Comparative overview of brain perfusion imaging techniques. Stroke 36:2032–2033. doi: 10.1161/01.STR.0000177839.03321.25
10. Smit EJ, Vonken E, van der Schaaf IC, et al. (2012) Timing-invariant reconstruction for deriving high-quality CT angiographic data from cerebral CT perfusion data. Radiology 263:216–25. doi: 10.1148/radiol.11111068
11. Beier J, Büge T, Stroszczynski C, et al. (1998) [2D and 3D parameter images for the analysis of contrast medium distribution in dynamic CT and MRI]. Radiologe 38:832–40. doi: 10.1007/s001170050431
12. Mendrik A, Vonken E-J, van Ginneken B, et al. (2010) Automatic segmentation of intracranial arteries and veins in four-dimensional cerebral CT perfusion scans. Med Phys 37:2956–2966. doi: 10.1118/1.3397813
13. Struffert T, Ott S, Kowarschik M, et al. (2013) Measurement of quantifiable parameters by time-density curves in the elastase-induced aneurysm model: first results in the comparison of a flow diverter and a conventional aneurysm stent. Eur Radiol 23:521–7. doi: 10.1007/s00330-012-2611-2
14. Klein S, Staring M, Murphy K, et al. (2010) elastix: a toolbox for intensity-based medical image registration. IEEE Trans Med Imaging 29:196–205. doi: 10.1109/TMI.2009.2035616
15. Sourbron S, Biffar AF, Ingrisch M, et al. (2009) PMI0.4: platform for research in medical imaging. Proc. ESMRMB, Antalya
16. R Core Team (2014) R: A Language and Environment for Statistical Computing.
17. Robin X, Turck N, Hainard A, et al. (2011) pROC: an open-source package for R and S+ to analyze and compare ROC curves. BMC Bioinformatics 12:77. doi: 10.1186/1471-2105-12-77
18. DeLong ER, DeLong DM, Clarke-Pearson DL (1988) Comparing the areas under two or more correlated receiver operating characteristic curves: a nonparametric approach. Biometrics 44:837–845. doi: 10.2307/2531595
19. Bonferroni C (1936) Teoria statistica delle classi e calcolo delle probabilita. Pubbl del R Ist Super di Sci Econ e Commer di Firenze 8:3–62.
20. Fisher RA (1936) THE USE OF MULTIPLE MEASUREMENTS IN TAXONOMIC PROBLEMS. Ann Eugen 7:179–188. doi: 10.1111/j.1469-1809.1936.tb02137.x
21. Biffar A, Baur-Melnyk A, Schmidt GP, et al. (2010) Multiparameter MRI assessment of normal-appearing and diseased vertebral bone marrow. Eur Radiol 20:2679–89. doi: 10.1007/s00330-010-1833-4
22. Schneider MJ, Cyran CC, Nikolaou K, et al. (2014) Monitoring early response to anti-angiogenic therapy: diffusion-weighted magnetic resonance imaging and volume measurements in colon carcinoma xenografts. PLoS One 9:e106970. doi: 10.1371/journal.pone.0106970
23. Gentleman RC, Carey VJ, Bates DM, et al. (2004) Bioconductor: open software development for computational biology and bioinformatics. Genome Biol 5:R80. doi: 10.1186/gb-2004-5-10-r80
24. Slawski M, Boulesteix A-L, Bernau C (2009) CMA: Synthesis of microarray-based classification.
25. Tan JC, Dillon WP, Liu S, et al. (2007) Systematic comparison of perfusion-CT and CT-angiography in acute stroke patients. Ann Neurol 61:533–43. doi: 10.1002/ana.21130
26. Miteff F, Levi CR, Bateman G a, et al. (2009) The independent predictive utility of computed tomography angiographic collateral status in acute ischaemic stroke. Brain 132:2231–8. doi: 10.1093/brain/awp155